Indian Journal of Biochemistry & Biophysics
Vol. 61, September 2024, pp. 527-538
DOI: 10.56042/ijbb.v61i9.10442

Computational investigation on the impact of point mutations on the N-terminal domain of SHANK3, indicating distinct synaptopathies in Autism spectrum disorder

Hiba Khalil Almaadani[#], and Venkata Satish Kumar Mattaparthi*

Molecular Modelling and Simulation Laboratory, Department of Molecular Biology and Biotechnology, Tezpur University, Tezpur-784 028, Assam, India

Received 20 April 2024; *revised 26 June 2024*

SHANK3 mutations are associated with a notable 1% of autism spectrum disorder (ASD). Due to the cost and time associated with experimental polymorphism studies, *in silico* investigations are deemed a rational precursor to elucidate the role of two mutations implicated in ASD, SHANK3 P141A and SHANK3 L270M. ASD is a complex neurological condition with diverse clinical manifestations, encompassing challenges in social interaction, communication, and repetitive behaviors. ASD is characterized by genetic heterogeneity, converging on a limited set of molecular pathways. Synaptopathies are one of the common neuronal processes associated with ASD, involving altered glutamatergic that may disrupt the excitatory and inhibitory equilibrium. SHANK3 is pivotal as a scaffold protein connecting glutamate receptors to the cytoskeleton, crucial for synaptic transmission within the post-synaptic density. We conducted a 200 ns molecular dynamics simulation to explore SHANK3 P141A and SHANK3 L270M functional and structural consequences on the SHANK3 protein. The P141A mutation significantly disrupted SHANK3 stabilization and caused a disturbance in intramolecular connections between SPN and ARR domains. The alteration affected the αCaMKII binding as one of the pivotal protein partners. On the contrary, the SHANK3 L270M mutation resulted in moderate stability conformation. The findings underscore the intricate dynamics of SHANK3 mutations and their potential relevance to the ASD.

Keywords: ASD, Molecular dynamics simulation, P141A and L270M mutations, SPN-ARR domains

Autism spectrum disorder (ASD) is a composite heterogeneous neurodevelopmental condition frequently characterized by a broad spectrum of clinical manifestations, including impairments in social and communicative interactions alongside restricted, repetitive behaviors. The current prevalence of ASD worldwide is estimated at 100/10,000[1]. A myriad of genetic loci have been implicated in pathomechanisms of ASD[2]; however, they converge to a few molecular pathways that have been engaged in the neurobiology of ASD[3], Synaptopathies are one of the common neuronal processes associated with ASD as a result of genetic variations during early brain construction, involved altered glutamatergic and GABAergic neurotransmission that may disrupt the excitatory and inhibitory equilibrium[4]. One pivotal protein that plays a role within the post-synaptic density (a microstructure housing the neurotransmitter reception system of excitatory synapses within the brain) of glutamatergic neurons is SH3 and multiple ankyrin repeat domains 3 structure (SHANK3)[5]; it binds the cytoskeleton in neuronal cells to glutamate receptors and thereby plays crucial role neurotransmission and integrity[6]. SHANK3 is present in the cortex and hippocampus. However, it seems to be dominantly expressed in the thalamus and striatum[7],located in chromosome 22q13.33. It consists of five distinct domains involving the Shank/ProSAP N-terminal domain (SPN), which constitutes one of the essential domains of SHANK3, the SPN domain adopts a conformation resembling a ubiquitin-like (Ubl) domain analogous to Ras association domains; consequently, previous investigations have demonstrated that activated Ras and Rap proteins exhibit heightened affinity for the SPN domain of SHANK3[8,9]. Moreover, the SPN region engages in close intramolecular interactions with the Ankyrin Repeat Region (ARR) or Ank domain, impeding accessibility of α-Fodrin and Sharpin as known interaction partners of the Ank repeat[10]. Furthermore,

[#]Equally contributed
*Correspondence:
Phone: 91-3712-275443, +91-8811806866 (Mob)
Fax: 91-3712-267005/267006
E-mail: mvenkatasatishkumar@gmail.com; venkata@tezu.ernet.in
Suppl. Data available on respective page of NOPR

the loop structure between SPN and ARR serves as a specific site for the interaction with Ca^{2+}/calmodulin-dependent kinase IIα (CaMKIIα), which partially conceals the Ras binding site. CaMKIIα, a crucial element in synaptic plasticity and learning processes, plays a pivotal role in decoding synaptic Ca^{2+} oscillations, regulating calcium levels, PSD integration, and shaping the morphology of dendritic spines[11]. In contrast, the SH3 domain connects with AMPARs are ionic channels that mediate fast synaptic transmission across the neuron's cell membrane in response to the neurotransmitter glutamate and contribute to processes like learning and memory[12]. Ultimately, within the SHANK3 protein, a proline-rich region is situated among the C-terminal SAM and PDZ domains[13], as exhibited in (Fig. 1). A wide range of neuropsychological and neurological developmental conditions, including ASD, have been linked to SHANK3 mutations[14]. Significantly, a notable 1% of individuals diagnosed with ASD exhibit diverse mutations in the SHANK3 gene, thereby classifying it as a high-risk gene associated with ASD[5,15]. Owji (2020)[16] discerned 29 deleterious missense variants within the SHANK3 gene, wherein mutations such as L47P, G54W, and G250D exhibited pronounced destabilizing effects. Molecular dynamics simulations were employed, revealing alterations in intramolecular interactions and heightened fluctuations in residues 1–350, particularly affecting the ARR functional domain. The N-terminal portion of SHANK3 has been impacted by multiple missense variants observed in ASD patients[16]. The relevance of these mutations concerning SHANK3 function and the pathogenesis of ASD remains unclear[17,18]. These results underscore the significance of further research on these mutations within the context of SHANK3.

A recent investigation unveiled a novel SHANK3 missense mutation (L270M) situated within the ARR domain, observed in individuals displaying an ADHD-like phenotype. Functional analysis elucidated that this mutation led to the loss of δ-catenin binding and disrupted intramolecular interactions, consequently influencing neurodevelopmental pathology[19]. An experimental investigation involving two cohorts of individuals with ASD identified the P141A mutation and hypothesized that it plays a pivotal function in the connection of SHANK3 to the membrane-associated cytoskeleton[18,19]. In addition, they have demonstrated its impact on the colocalization of SHANK3 with other postsynaptic density (PSD) proteins[20]and its association with reduced induction and maturation of dendritic spines[17]. Noteworthy, the experimental polymorphism research are cost-prohibitive and time-consuming. In light of this, the computational approach to analyzing functional mutations has been thought to be a sensible strategy for comprehending the structural and functional implications of these polymorphisms and their impacts on the structure and stability of the SHANK3 protein. To this end, our study aims to investigate two mutations that have been found in ASD patients, namely P141A and L270M mutants, in comparison to SHANK3 WT using molecular dynamics (MD) simulations to assess the stability of SHANK3 WT, SHANK3 L270M and SHANK3 P141A structures by examining protein equilibrium, flexibility, compactness, and intramolecular interactions. Consequently, to gain insights into the potential effects of deleterious mutation on the protein binding sites implicated in neuronal transaction associated with ASD pathogenesis.

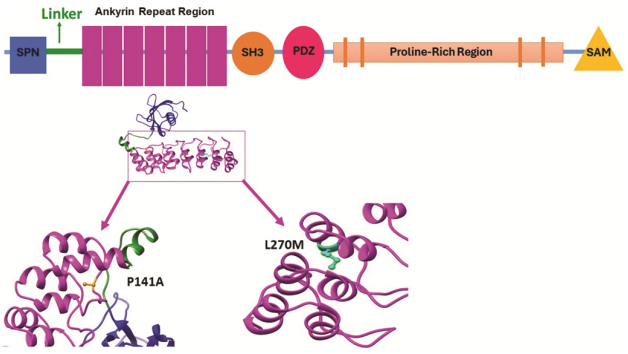

Fig. 1 — The domain architecture of SHANK3. The positions of the N-terminal mutations subjected to MD simulation are highlighted

Materials and Methods

Preparation of initial structures

SHANK3 protein

The SHANK3 structure, PDB ID 5G4X[8,21,22], was downloaded from the RCSB Protein Data Bank[23,24] and was utilized for molecular dynamics simulation.

Constructing the missense mutantsSHANK3 L270M and SHANK3 P141A

The primary structure of the SHANK3 L270M and P141Amutants was constructed by altering the 3D structure of the scaffold protein SHANK3 WT (PDB ID: 5G4X). The Rotamer tool of the CHIMERA software[25] was applied to generate SHANK3 L270M, where Leucine was substituted with Methionine at position 270 in the SHANK3. In contrast, SHANK3 P141A was constructed by substituting Proline with Arginine at position 141 in the ARR domain of SHANK3.

Setup for Molecular Dynamics simulations

SHANK3 L270M, P141A, and SHANK3 wild type (WT) systems were constructed for the MD simulation utilizing ff99SBildn as a force field parameter in the Leap module of the AMBER 14 software package[26]. The commonly used TIP3P water model[27] was applied as a solvent to explicitly stated SHANK3 WT and SHANK3 L270M, P141A mutant systems independently utilizing a buffer dimension of 10 Å in a periodic cubic box. The charge of the SHANK3 WT and the two SHANK3 L270M, P141A mutants structures have been neutralized by the addition of an adequate number of counter ions and afterwards, undergoing a reduction of energy to exclude the London dispersion force.

The molecular dynamics simulation adheres to a consistent method comprising heating dynamics followed by density, equilibrium, and production dynamics. Initial structures were energy-minimized for further Molecular Dynamics procedures. The gradual heating of structures from 0 to 300 K occurred under a constant volume (NVT) situation, followed by the density approach. Equilibration was accomplished under NPT conditions (300 K and 1 atm pressure) for one nanosecond. Visualization and analysis of energy, temperature, and pressure were undertaken to ensure correct equilibration, as depicted in (Suppl. Fig. 1A-C) for SHANK3 WT, and (Suppl. Fig. 2A-C) for SHANK3 L270M mutant, as well as (Suppl. Fig. 3A-C) for SHANK3 P141A mutant. Subsequently, a 200 ns MD production run for stabilized structures using the PME algorithm[28,29] with a time step of 2 fs. A threshold of 8 Å addressed nonbonding connections, whereas, electrostatic forces were managed using the PME technique. The SHAKE algorithm restricted all bonds[28]while temperature and pressure were maintained stationary *via* the Berendsen weak coupling algorithm mover the simulation[30]. Snapshots were taken through the trajectory at intervals of 10 ns for further investigations of each structure.

The PTRAJ and CPPTRAJ modules of AmberTools 14 were applied to analyze molecular dynamics trajectories of both the SHANK3 WT and the two SHANK3 L270M, P141A mutants[28] of AmberTools 14. To evaluate the convergent behavior of our structures, the RMSDs for SHANK3 WT and the two SHANK3 L270M, P141A mutants have been analyzed, wherein the initial MD system was employed as the template for analysis.

Besides that, the three structures underwent radius gyration, hydrophobic interactions, and intramolecular distance analysis. The analysis of intra-molecular hydrogen bonds was performed for SHANK3 WT and the two SHANK3 L270M, P141A mutants according to the potential donors (HD) and acceptors (HA) of the protons. UCSF Chimera software[25] was utilized to depict the 3D structure of each system. The xmgrace plotting tools were applied to generate the plots. The monitoring of pressure, temperature, kinetic energy, total energy, and potential energy, was systematically validated throughout the simulation time for the SHANK3 WT and the two SHANK3 L270M, P141A SHANK3 mutants systems.

The docking between the three structures, SHANK3 WT and the two SHANK3 L270M, P141A SHANK3 mutants with protein partner αCaMKII, was conducted using a ClusPro (protein-protein docking) server[31-33], and the results were analyzed through the PDBsum server[34].

Results and Discussion

The root mean square deviation (RMSD)

RMSD analysis of atomic distances was performed over a 200 ns simulation period encompassing the SHANK3 WT protein, along with the SHANK3 L270M and P141A mutants. This analysis provided valuable insights into their conformational dynamics[35]. The RMSD of the SHANK3 WT protein exhibited a gradual increase, marked by initial fluctuations, followed by a notable transition around 3.9 Å, ultimately stabilizing towards the conclusion of the simulation (Fig. 2A). Conversely, the SHANK3 L270M mutant displayed a sudden increase in RMSD with fluctuations, characterized by intense dynamic at 3.7 Å, followed by a decrease in RMSD, then later stabilized to the end of the simulation (Fig. 2C). Similarly, the SHANK3 P141A mutant exhibited an abrupt increase in RMSD, followed by fluctuations and another impulse at 4.2 Å, then a gradual increase beyond 150 ns (Fig. 2E). These results suggest that the SHANK3 WT and SHANK3 L270M mutant could be slightly stable compared to the SHANK3 P141A mutant, which might have high structure flexibility. To discern the domain that contributes to these conformational changes, RMSD analyses were conducted for the three domains SPN, ARR, and Linker separately. Notably, RMSD traces restricted to the SPN and ARR domains revealed the same pattern

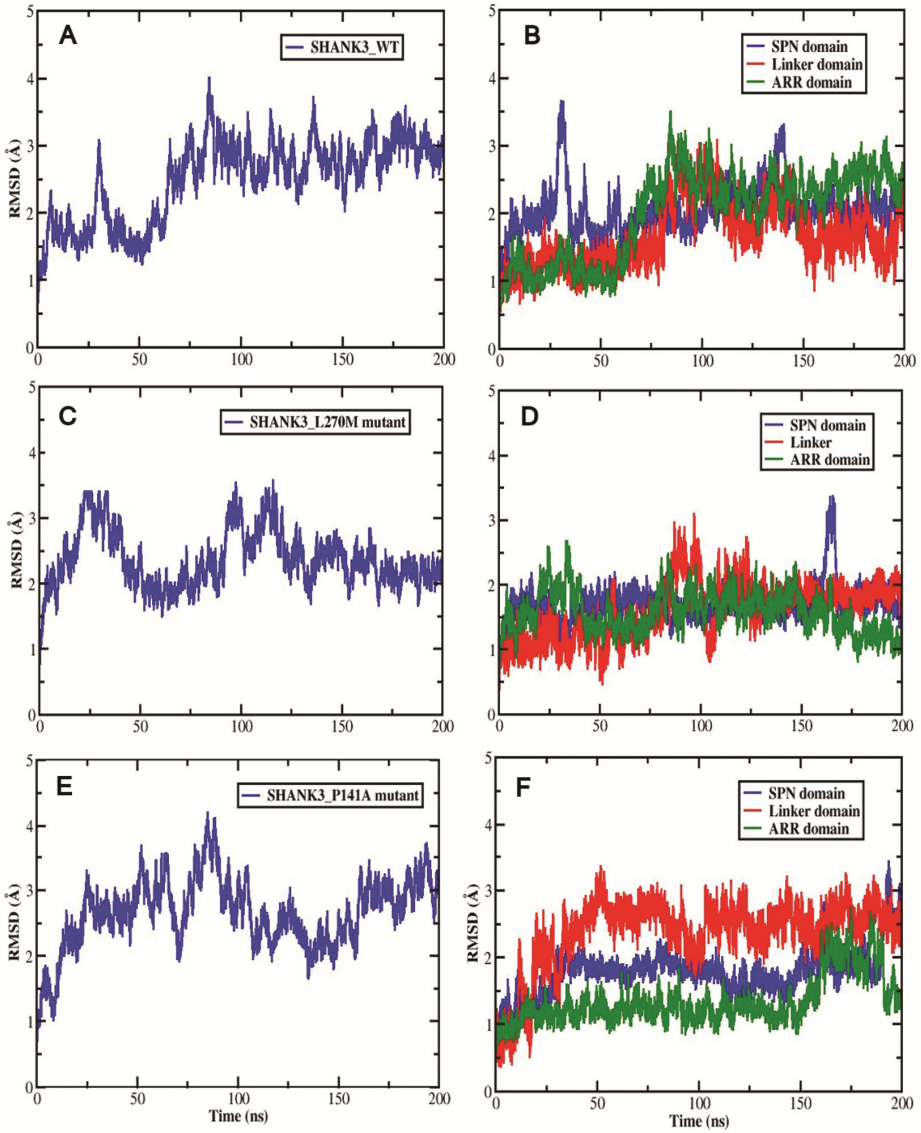

Fig. 2 — The plot of RMSD for (A) SHANK3 WT protein; (B)Three domains in SHANK3 WT; (C)SHANK3 L270M mutant; (D) Three domains in SHANK3 L270M mutant; (E) SHANK3 P141A mutant; and (F) Three domains in SHANK3 P141A mutant

noticed for the SHANK3 WT protein (Fig. 2B). The SHANK3 L270M mutant also revealed no significant RMSD related to a specific domain (Fig. 2D). In contrast, the SPN and Linker domains in the SHANK3 P141A mutant revealed distinctively increased fluctuations, suggesting their potential involvement in constitutional modifications, as exhibited in (Fig. 2F).

The root mean square fluctuation (RMSF)

The results of RMSF demonstrated slightly increased conformational flexibility in the SHANK3 WT compared to the two mutants SHANK3 L270M and P141A (Fig. 3A, C, and E), respectively. Noteworthy was the flexibility observed in amino acid residues corresponding to the SHANK3 SPN and Linker domains in SHANK3 WT and the two mutants, as depicted in (Fig. 3B, D, and F). Hence, it can be inferred that the SPN and Linker domains may possess functional significance owing to their elevated RMSF values.

The radius of gyration (Rg) analysis

The radius of gyration (Rg) is a frequently employed metric for assessing the spatial distribution of atoms within a specific biological molecule, measured from the principal center of gravity[36]. The radius of gyration is utilized to monitor changes in structural compactness and folded over simulation time. According to the Rg plots, the SHANK3 WT

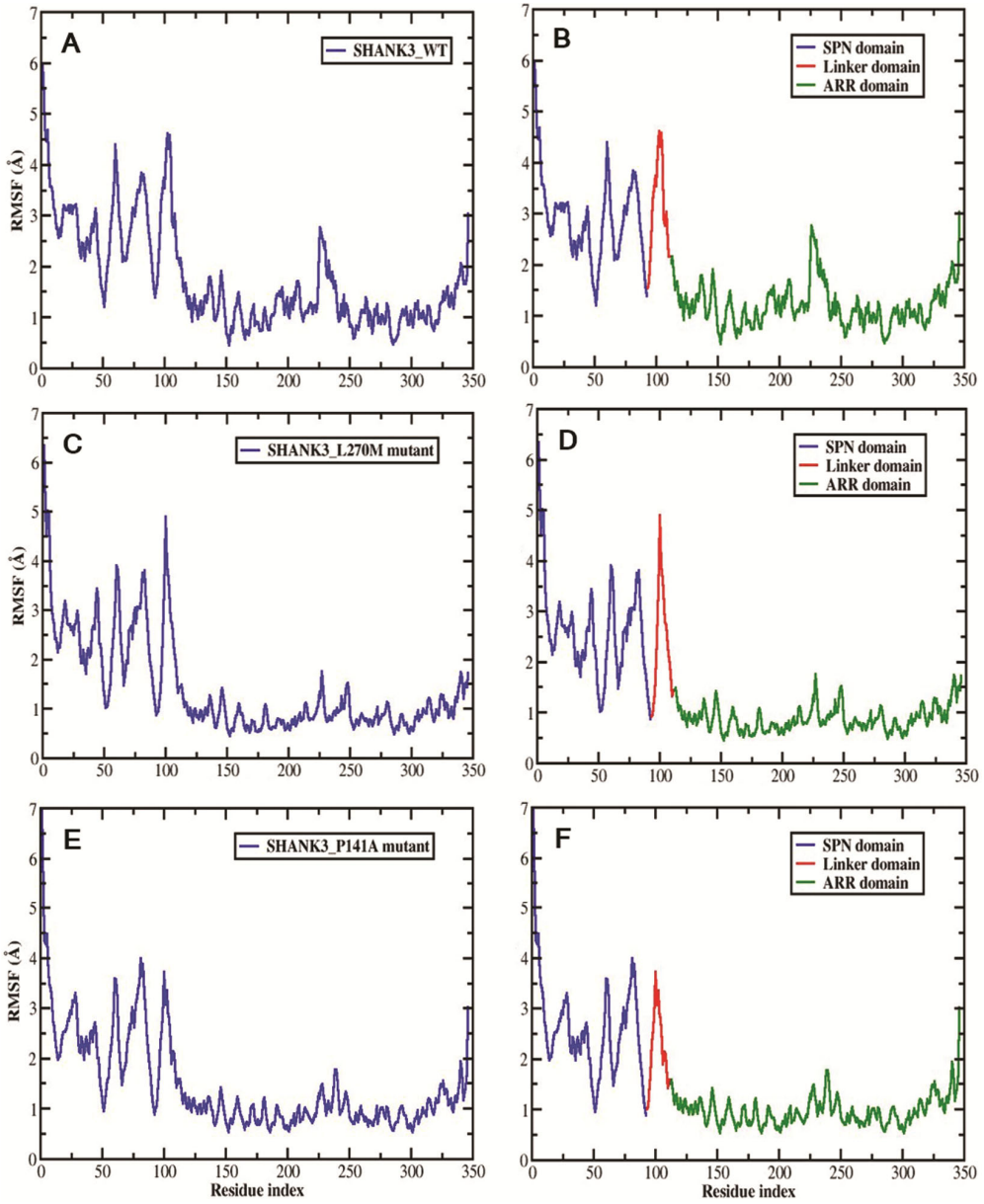

Fig. 3 — RMSF plots for the (A) SHANK3 WT protein; (B) Three domains in SHANK3 WT; (C) SHANK3 L270M mutant; (D) Three domains in SHANK3 L270M mutant; (E) SHANK3 P141A mutant; and (F) Three domains in SHANK3 P141A mutant

protein disclosed lower values over time of the simulation of 200 ns comparison to the L270M and SHANK3 P141A mutants, as exhibited in (Fig. 4A-C, respectively). Notably, the SHANK3 P141A mutant has the highest Rg values throughout the simulation; therefore, theSHANK3 P141A mutant refers to a less compact and unfolded state. Noteworthy, the SHANK3 L270M mutation is positioned within the hydrophobic part of the ARR domain without displaying significant characteristics of an unfolding state, as the majority of the interactions within the SHANK3 N-terminal region remain preserved[19].

Observed reduction in δ-catenin binding which contributed to the relatively milder ASD phenotype. Thereby, the plausible interpretation from previous study and our findings that the SHANK3 L270M mutation subtly modifies the surface characteristics of the ARR domain in a manner incompatible with δ-catenin binding. Herein, it is worth noting thatloss-of-function mutations in the CTNND2 gene that encodes δ-catenin have been linked to an ADHD phenotype[37]. Consequently, further experimental investigations are required to elucidate the impact of the SHANK3 L270M in ASD.

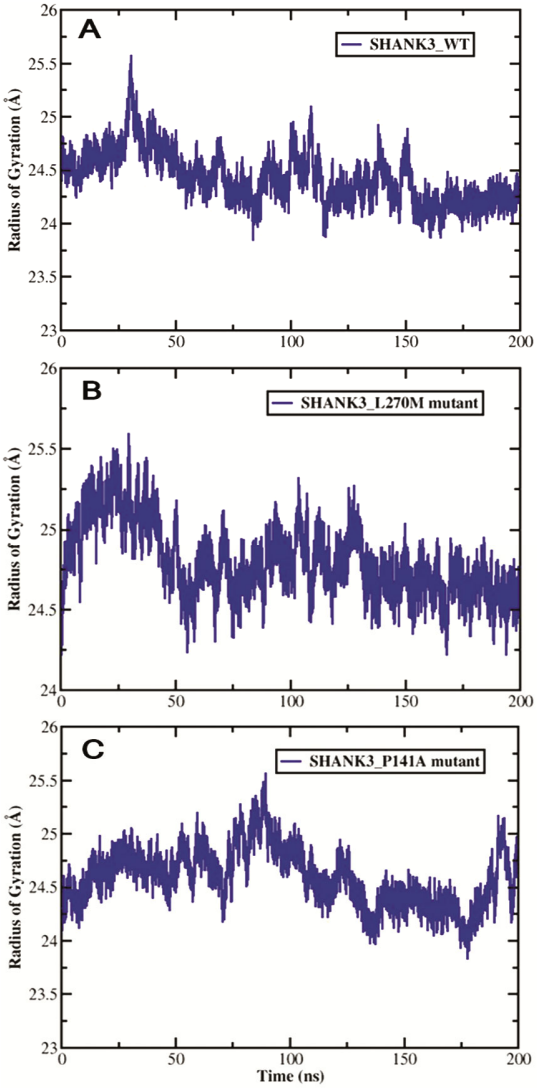

Fig. 4 — The radius of gyration plots (A) SHANK3 WT protein; (B) SHANK3 L270M mutant; and (C) SHANK3 P141A mutant. The time in the ns is on the x-axis, whereas Rg is on the y-axis

Analysis of the distance between center of mass SPN and ARR domains

The central point of mass distance between the SPN-ARR domains of SHANK3 WT and the two mutants SHANK3 L270M and P141A was assessed. The distance between SPN-ARR in the SHANK3 WT protein increased initially, followed by a sudden reduction (Fig. 5A). Conversely, the SHANK3 L270M mutant exhibited an initial increase in distance, gradually decreasing to a conserved state between the two domains (Fig. 5B). In contrast, the SHANK3 P141A mutant showed a continuous increase in distance, suggesting an impact on domain interactions and the potential open-up of the SPN-ARR fold over time (Fig. 5C).

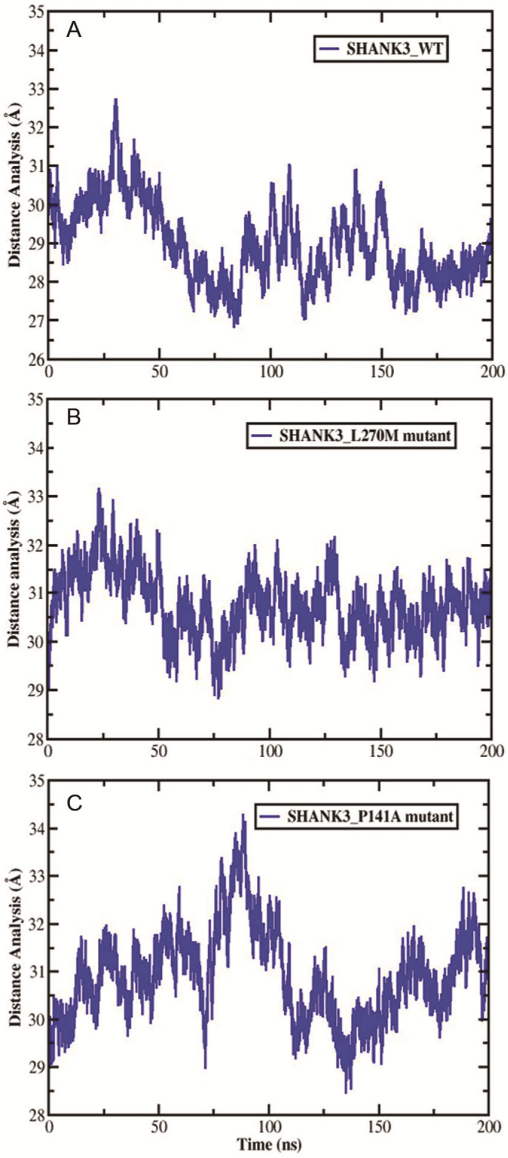

Fig. 5 — The distance between SPN and ARR domains analysis (A) SHANK3 WT protein; (B) SHANK3 L270M mutant; and (C) SHANK3 P141A mutant

Intra-molecular hydrogen bond analysis

Intramolecular hydrogen bonds were quantified to assess the proximity of all-atom interactions within the SHANK3 WT protein and its two mutants, SHANK3 L270M and P141A. These intramolecular hydrogen bond contacts serve as pivotal metrics for gauging the structural compactness within the distinct domains of the SHANK3 WT protein. The results revealed an increase in intra-molecular interactions in the SHANK3 WT protein in comparison with the SHANK3 L270M and SHANK3 P141A mutants, with the lowest number of hydrogen bonds observed in the SHANK3 P141A mutant, as illustrated in (Fig. 6A1,

B1, and C1). Similarly, the SPN domain exhibited higher disparities in the SHANK3 WT protein compared to the SHANK3 L270M and SHANK3 P141A mutants (Fig. 6A2, B2, and C2). Furthermore, the ARR domain displayed fewer intramolecular hydrogen bonds in the SHANK3 P141A mutant than in the SHANK3 WT protein and SHANK3 L270M mutant, as depicted in (Fig. 6A4, B4, and C4). Conversely, the Linker domain showed no significant differences between the SHANK3 WT protein, SHANK3 L270M, and SHANK3 P141A mutants, as illustrated in (Fig. 6A3, B3, and C3).

Our findings indicated that the SHANK3 WT protein has a heightened level of molecular interactions within the SPN and ARR regions, linking to the overall stability of the protein and maintaining a closed conformation, as shown previously in (Fig. 4A). Conversely, the SHANK3 P141A mutant knocked down the intramolecular connections between SPN and ARR, consequently significantly opening up the distance between SPN and ARR regions, as depicted in (Fig. 5C). Numerous investigations have been initiated to unravel the functional importance of the intramolecular connections between SPN and ARR[38] and their implications in the pathogenesis of ASD.

Recent reports have highlighted the involvement of the linker domain connecting both regions, along with

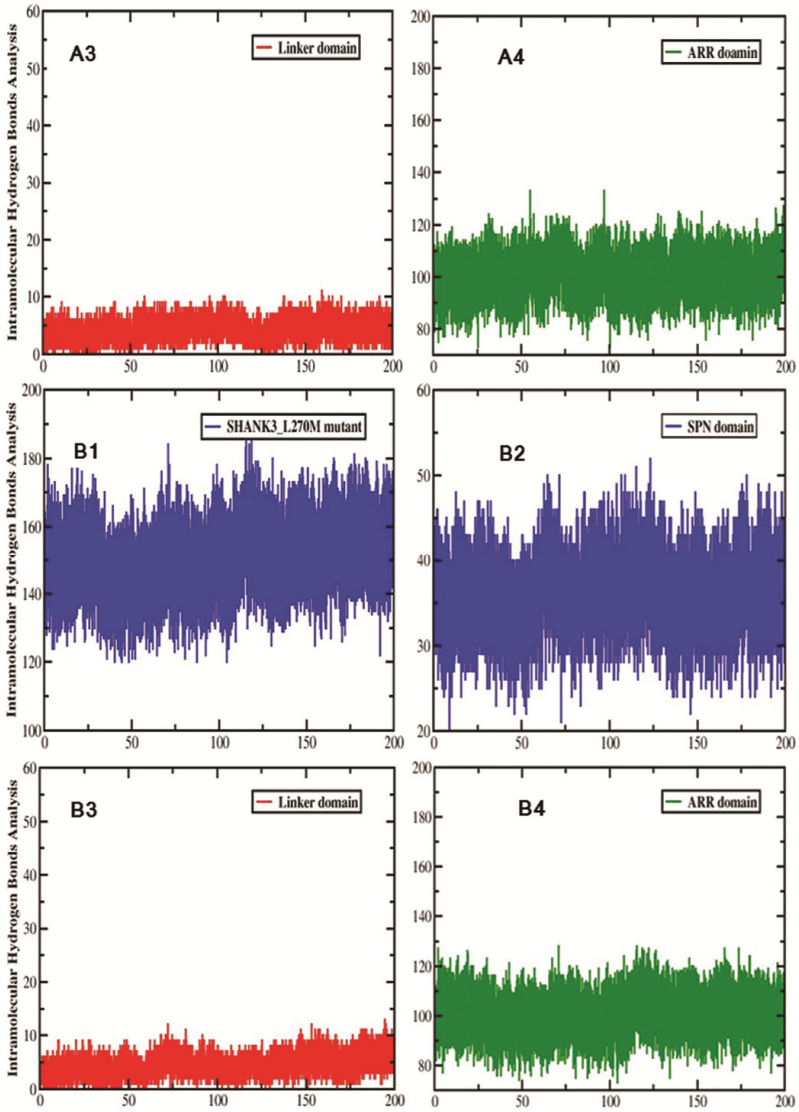

Fig. 6 — The intramolecular hydrogen bonds analysis (A1) SHANK3 WT protein; (A2) WT SPN domain; (A3) WT Linker domain; (A4) WT ARR domain; (B1) SHANK3 L270M mutant; (B2) L270M SPN domain; (B3) L270M Linker domain; (B4) L270M ARR domain; (C1) SHANK3 P141A mutant; (C2) P141A SPN domain; (C3) P141A Linker domain; and (C4) P141A ARR domain

(*Contd.*)

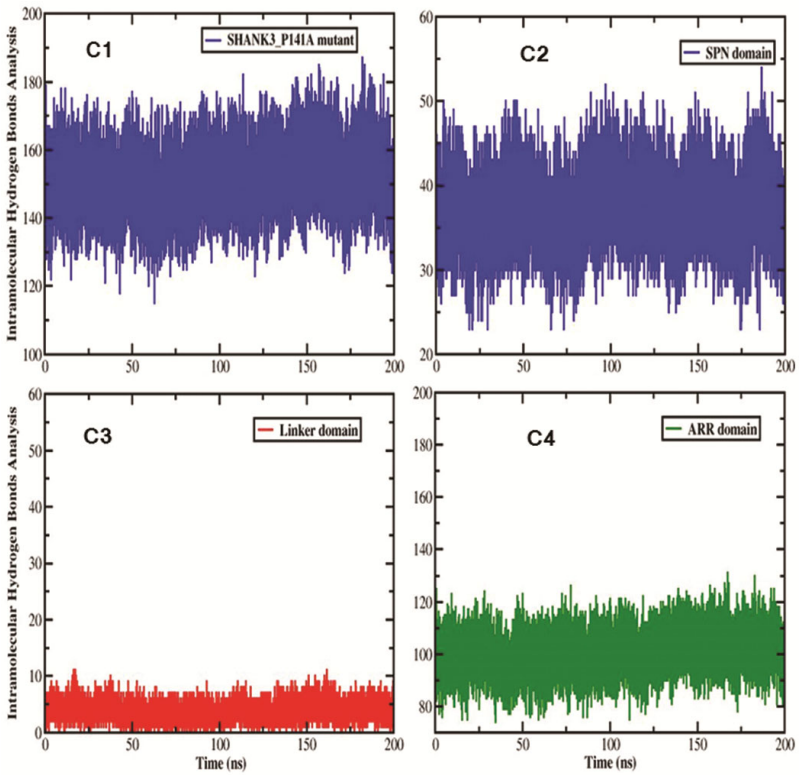

Fig. 6 — The intramolecular hydrogen bonds analysis (A1) SHANK3 WT protein; (A2) WT SPN domain; (A3) WT Linker domain; (A4) WT ARR domain; (B1) SHANK3 L270M mutant; (B2) L270M SPN domain; (B3) L270M Linker domain; (B4) L270M ARR domain; (C1) SHANK3 P141A mutant; (C2) P141A SPN domain; (C3) P141A Linker domain; and (C4) P141A ARR domain

a segment of the SPN, in establishing a binding surface for αCaMKII. This binding occurs in its inactive state, non-phosphorylated, and requires a closed configuration of the SPN-ARR tandem[11,19]. Consequently, disrupting the intramolecular interactions between SPN and ARR regions may induce a conformational change in the Linker domain, resulting in reduced affinity to αCaMKII. In agreement with previously reported results[11,19] our findings, as seen from (Suppl. Table 1) and (Suppl. Figs 4A and 5A), indicated that the interaction between the SHANK3 WT protein and αCaMKII exhibits higher affinity in comparison to those predicted for the SHANK3 P141A mutant with αCaMKII (see Suppl. Table 2 & Suppl. Figs 4B and 5B). Unlike that, the SHANK3 L270M mutant has exhibited a lower affinity, as seen in (Suppl. Figs 4C and 5C) as well as (Suppl. Table 3). Hence, a plausible conjecture regarding the SHANK3 L270M mutation arises from its location within the ARR domain, which does not constitute a binding site for αCaMKII.

Also, it should be noted that the distinctive interaction between αCaMKII and SHANK3 plays a pivotal role in instigating a specialized long-range signaling pathway from the plasma cell membrane to the nucleus, and this is true specifically for L-type calcium channels (LTCCs). This signaling mechanism is imperative for inducing activity-dependent alterations in neuronal gene transcription during the processes of memory and learning[39]. It was previously reported in the literature that the disruption of αCaMKII activity emerges as a prevalent process, generating modifications to the structure of glutamatergic and plasticity neuron function, contributing to the pathogenesis of neurological disorders[40].

Conversely, an earlier research indicates that intramolecular interaction prevents α-Fodrin to access its location on the ARR domain in SHANK3 WT while SHANK3 P141A significantly boosts the connecting of α-Fodrin to SHANK3[19,41]. Considering our findings, which indicate that SHANK3 P141A disrupts the connections between SPN-ARR domains, one may indicate a potential scenario in which the open conformation facilitates α-Fodrin binding, increases actin linkage and enhances integrin

activation. Taken together, these mutants might change the flexible conformation of SHANK3, leading to an impairment of the capacity to coordinate cytoskeletal aggregation and signaling dysregulation. The physiological activity of the SHANK3-actin connection influences dendritic protrusion morphology in neuron cells and ASD-related characteristics *in vivo*[42]. Notably, SHANK3 loss-of-function mutations have been associated with neurodevelopmental diseases such as ASD[43].

Intermolecular hydrogen bonds analysis

The interaction between the SPN and ARR domains was investigated through hydrogen bonds. The findings revealed that the SHANK3 WT protein exhibited more hydrogen bonds than the SHANK3 L270M mutant and SHANK3 P141A mutant, as shown in (Fig. 7A-C, respectively), indicating more stability.

Secondary structure analysis

The Kabsch and Sander algorithm[44,45] within the DSSP program was employed for secondary structure analysis of the three structures of SHANK3 WT protein and the two mutants, SHANK3 L270M and P141A. The plots depicting the results for the secondary structure analysis for the SHANK3 WT protein are presented in (Fig. 8A)and the SHANK3 L270M mutant, as shown in (Fig. 9A), as well as for the SHANK3 P141A mutant (Fig. 10A). In addition (Suppl. Fig 6A-C) shows the secondary structure SHANK3 WT protein for three domains and SHANK3 L270M (Suppl. Fig 7A-C), and secondary structure SHANK3 P141A for three domains as illustrated in (Suppl. Fig 8A-C). The graphics

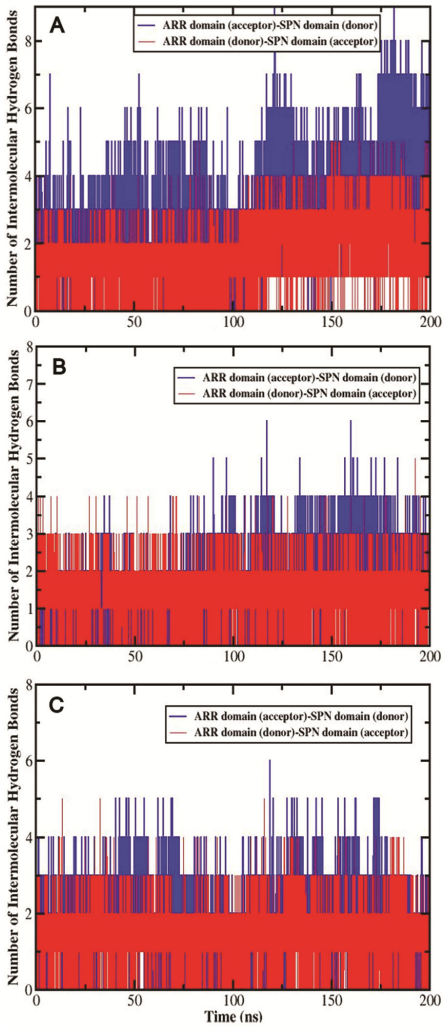

Fig.7 — The number of H-bonds between SPN-ARR domains for 200 ns MD simulation (A) SHANK3 WT; (B) SHANK3 L270M mutant; and (C) SHANK3 P141A mutant

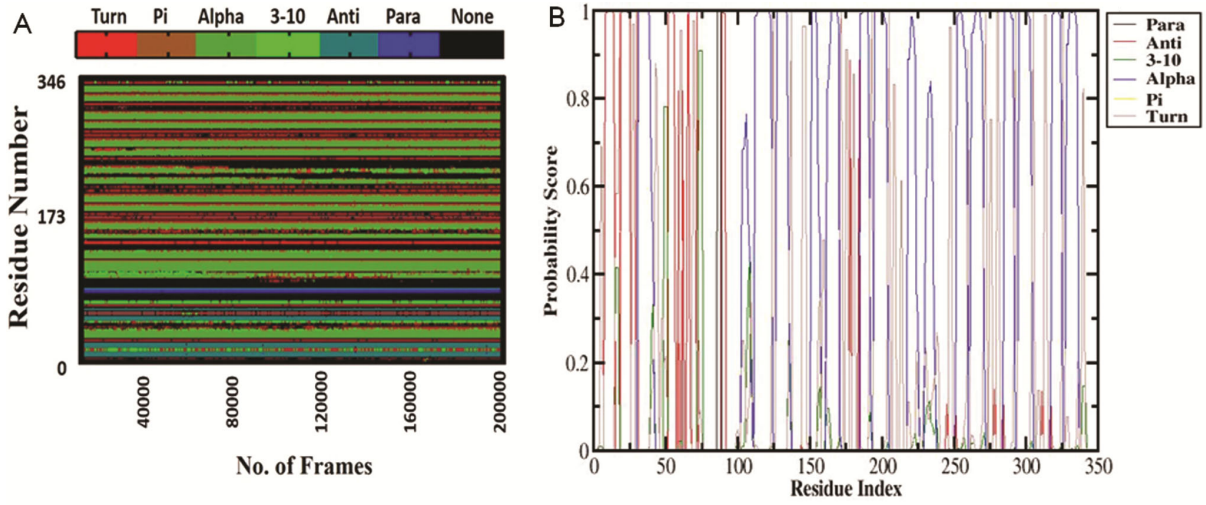

Fig. 8 — Secondary structure analysis (A) SHANK3 WT Protein. Secondary structure probability score of residue index; and (B) SHANK3 WT protein

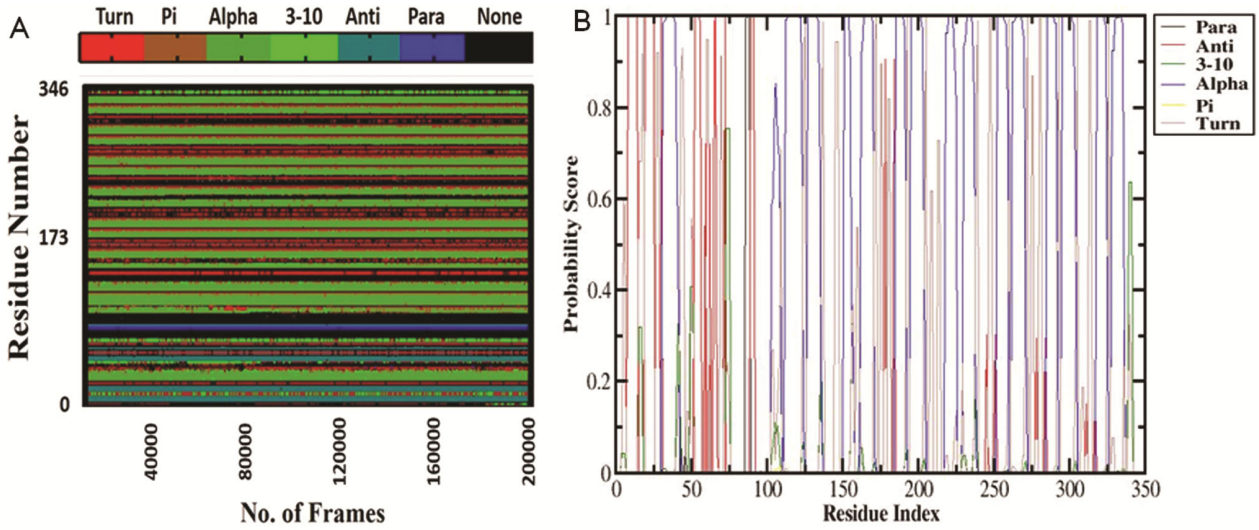

Fig. 9 — Secondary structure analysis (A) SHANK3 L270M mutant. Secondary structure probability score of residue index; and (B) SHANK3 L270M mutant

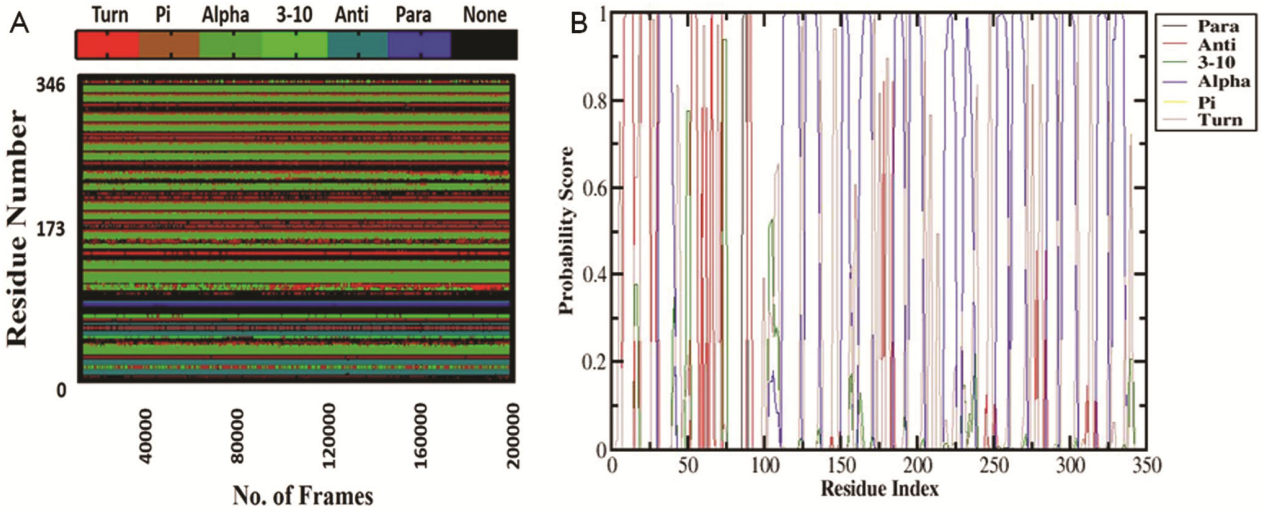

Fig. 10 — Secondary structure analysis (A) SHANK3 P141A mutant. Secondary structure probability score of residue index; and (B) SHANK3 P141A mutant

represent the variability of secondary structure across each residue as an indication of frame numbers. In addition, the proportion content of individual secondary structures in the SHANK3 WT protein, SHANK3 L270M, and SHANK3 P141A mutants was determined over their respective average structures generated in 200 ns MD simulations, which were carried out by using YASARA software[46,47]. The findings indicate that the SHANK3 L270M mutant and SHANK3 P141A mutant exhibit a higher helical content than the SHANK3 WT protein do, as seen from (Suppl. Table 4). We conducted an assessment of the secondary structure probability assumed by the SHANK3 WT and two variants, namely SHANK3 L270M and SHANK3 P141A mutants, employing quantitative measures as a function of residue index, as delineated in (Fig. 8B) for SHANK3 WT protein and (Suppl. Fig 6D-F) for three domains (Fig. 9B) presents the SHANK3 L270M mutant and (Suppl. Fig 7D-F) for three domains, as well as SHANK3 P141A mutant as shown in (Fig. 10B) and (Suppl. Fig 8D-F).

Conclusion

In conclusion, our study extensively investigated the role of SHANK3 P141A and SHANK3 L270M mutants within the SHANK3 gene, particularly in the N-terminal region. The SHANK3 P141A mutant exhibited a significant impact, hindering the

stabilization and folding of SHANK3, as well as disrupting intramolecular interactions between SPN and ARR, influencing its binding with αCaMKII, which will have a significant impact on synaptic functionality and might play a potential role in ASD. In contrast, the SHANK3 L270M mutant exhibited a moderate stability and lesser intramolecular hydrogen bonding when compared to the SHANK3 WT mutant. These findings emphasize the intricate dynamics of SHANK3 mutations and suggest that their potential contributions to neurodevelopmental disorders such as ASD, warranting further computational and experimental investigations to elucidate their precise role in ASD pathogenesis.

Acknowledgement

The authors extend their deepest gratitude to Department of Molecular Biology and Biotechnology, Tezpur University for providing computing facility and University GrantsCommission, India, for the start-up grant. Hiba Almaadani extends her gratitude to Indian Council for Cultural Relations (ICCR) for the scholarship to pursue PhD programme at Tezpur University.

Conflict of interest

Both the authors declare no conflict of interest.

References

1 Zeidan J, Fombonne E, Scorah J, Ibrahim A, Durkin MS, Saxena S, Yusuf A, Shih A & Elsabbagh M, Global prevalence of autism: A systematic review update. *Autism Res,* 15 (2022) 778.

2 Ghafouri-Fard S, Pourtavakoli A, Hussen B M, Taheri M & Ayatollahi SA, A Review on the Role of Genetic Mutations in the Autism Spectrum Disorder. *Mol Neurobiol,* 60 (2023) 5256.

3 Alonso-Gonzalez A, Rodriguez-Fontenla C & Carracedo A, De novo mutations (DNMs) in autism spectrum disorder (ASD): Pathway and network analysis. *Front Genet,* 9 (2018) 1.

4 Molloy CJ, Cooke J, Gatford NJ, Rivera-Olvera A, Avazzadeh S, Homberg JR, Grandjean J, Fernandes C, Shen S & Loth E, Bridging the translational gap: what can synaptopathies tell us about autism? *Front Mol Neurosci,* 16 (2023) 1.

5 Monteiro P & Feng G, SHANK proteins: roles at the synapse and in autism spectrum disorder. *Nat Rev Neurosci,* 18 (2017) 147.

6 Ivashko-Pachima Y, Ganaiem M, Ben-Horin-Hazak I, Lobyntseva A, Bellaiche N, Fischer I, Levy G, Sragovich S, Karmon G & Giladi E, SH3-and actin-binding domains connect ADNP and SHANK3, revealing a fundamental shared mechanism underlying autism. *Mol Psychiatry*, 27 (2022) 3316.

7 Sheng M & Kim E, The Shank family of scaffold proteins. *J Cell Sci,* 113 (2000) 1851.

8 Lilja J, Zacharchenko T, Georgiadou M, Jacquemet G, Franceschi N D, Peuhu E, Hamidi H, Pouwels J, Martens V & Nia FH, SHANK proteins limit integrin activation by directly interacting with Rap1 and R-Ras. *Nat Cell Biol,* 19 (2017) 292.

9 Cai Q, Hosokawa T, Zeng M, Hayashi Y & Zhang M, Shank3 binds to and stabilizes the active form of Rap1 and HRas GTPases via Its NTD-ANK tandem with distinct mechanisms. *Structure*, 28 (2020) 290.

10 Nia FH, Woike D, Martens V, Klüssendorf M, Hönck HH, Harder S & Kreienkamp HJ, Targeting of δ-catenin to postsynaptic sites through interaction with the Shank3 N-terminus. *Mol Autism*, 11 (2020) 1.

11 Cai Q, Zeng M, Wu X, Wu H, Zhan Y, Tian R & Zhang M, CaMKIIα-driven, phosphatase-checked postsynaptic plasticity via phase separation. *Cell Res,* 31 (2021) 37.

12 Chiu SL, Chen CM & Huganir RL, ICA69 regulates activity-dependent synaptic strengthening and learning and memory. *Front Mol Neurosci,* 16 (2023) 1.

13 Vyas Y & Montgomery JM, The role of postsynaptic density proteins in neural degeneration and regeneration. *Neural Regen Res,* 11 (2016) 906.

14 Peça J, Feliciano C, Ting J T, Wang W, Wells MF, Venkatraman TN, Lascola CD, Fu Z & Feng G, Shank3 mutant mice display autistic-like behaviours and striatal dysfunction. *Nature*, 472 (2011) 437.

15 Barak B & Feng G, Neurobiology of social behavior abnormalities in autism and Williams syndrome. *Nat Neurosci,* 19 (2016) 647.

16 Owji H, Eslami M, Nezafat N & Ghasemi Y, *In silico* elucidation of deleterious non-synonymous SNPs in SHANK3, the autism spectrum disorder gene. *J Mol Neurosci,* 70 (2020) 1649.

17 Durand C M, Perroy J, Loll F, Perrais D, Fagni L, Bourgeron T, Montcouquiol M & Sans N, SHANK3 mutations identified in autism lead to modification of dendritic spine morphology *via* an actin-dependent mechanism. *Mol Psychiatry*, 17 (2012) 71.

18 Boccuto L, Lauri M, Sarasua SM, Skinner C D, Buccella D, Dwivedi A, Orteschi D, Collins J S, Zollino M & Visconti P, Prevalence of SHANK3 variants in patients with different subtypes of autism spectrum disorders. *Eur J Hum Genet,* 21 (2013) 310.

19 Woike D, Wang E, Tibbe D, Nia FH, Failla AV, Kibæk M, Overgård TM, Larsen M J, Fagerberg CR & Barsukov I, Mutations affecting the N-terminal domains of SHANK3 point to different pathomechanisms in neurodevelopmental disorders. *Sci Rep,* 12 (2022) 902.

20 Moessner R, Marshall CR, Sutcliffe JS, Skaug J, Pinto D, Vincent J, Zwaigenbaum L, Fernandez B, Roberts W & Szatmari P, Contribution of SHANK3 mutations to autism spectrum disorder. *Am J Hum Genet,* 81 (2007) 1289.

21 Kumar A, Mishra T & Kulshreshtha A, Binding interaction of laccases from *Bacillus Subtilis* after industrial dyes exposure: Molecular docking and molecular dynamics simulation studies. *Indian J Biochem Biophys,* 60 (2023) 320.

22 Ramakrishnan P, Pandi P, Jothimani M, Sundaravel SS, Muthusamy K, Narayanan U, Pannipara M, Al-Sehemi AG & Jayaraman A, Computational approach on *Moringa oleifera* as an inhibitor against SARS-CoV-2 structural proteins. *Indian J Biochem Biophys,* 60 (2023) 941.

23 Berman HM, Westbrook J, Feng Z, Gilliland G, Bhat TN, Weissig H, Shindyalov IN & Bourne PE, The protein data bank. *Nucleic Acids Res,* 28 (2000) 235.

24 Rose PW, Prlić A, Bi C, Bluhm WF, Christie CH, Dutta S, Green RK, Goodsell DS, Westbrook JD & Woo J, The RCSB Protein Data Bank: views of structural biology for basic and applied research and education. *Nucleic Acids Res,* 43 (2015) D345.

25 Pettersen EF, Goddard TD, Huang CC, Couch GS, Greenblatt DM, Meng EC & Ferrin TE, UCSF Chimera—a visualization system for exploratory research and analysis. *J Comput Chem,* 25 (2004) 1605.

26 Henriques J, Cragnell C & Skepo M, Molecular dynamics simulations of intrinsically disordered proteins: force field evaluation and comparison with experiment. *J Chem Theory Comput,* 11 (2015) 3420.

27 Jorgensen WL, Chandrasekhar J, Madura JD, Impey RW & Klein ML, Comparison of simple potential functions for simulating liquid water. *J Chem Phys,* 79 (1983) 926.

28 Ryckaert JP, Ciccotti G & Berendsen HJ, Numerical integration of the cartesian equations of motion of a system with constraints: molecular dynamics of n-alkanes. *J Comput Phys,* 23 (1977) 327.

29 Salomon-Ferrer R, Gotz AW, Poole D, Le Grand S & Walker RC, Routine microsecond molecular dynamics simulations with AMBER on GPUs. 2. Explicit solvent particle mesh Ewald. *J Chem Theory Comput,* 9 (2013) 3878.

30 Berendsen HJ, Postma JV, Van Gunsteren WF, DiNola A & Haak JR, Molecular dynamics with coupling to an external bath. *J Chem Phys,* 81 (1984) 3684.

31 Comeau SR, Kozakov D, Brenke R, Shen Y, Beglov D & Vajda S, ClusPro: performance in CAPRI rounds 6–11 and the new server. *Proteins*, 69 (2007) 781.

32 Kozakov D, Beglov D, Bohnuud T, Mottarella SE, Xia B, Hall DR & Vajda S, How good is automated protein docking? *Proteins*, 81 (2013) 2159.

33 Kozakov D, Hall DR, Xia B, Porter KA, Padhorny D, Yueh C, Beglov D & Vajda S, The ClusPro web server for protein–protein docking. *Nat Protoc,* 12 (2017) 255.

34 Laskowski RA, Jabłońska J, Pravda L, Vařeková RS & Thornton JM, PDBsum: Structural summaries of PDB entries. *Protein Sci,* 27 (2018) 129.

35 Knapp B, Frantal S, Cibena M, Schreiner W & Bauer P, Is an intuitive convergence definition of molecular dynamics simulations solely based on the root mean square deviation possible? *J Comput Biol,* 18 (2011) 997.

36 Falsafi-Zadeh S, Karimi Z & Galehdari H, VMD DisRg: New User-Friendly Implement for calculation distance and radius of gyration in VMD program. *Bioinformation*, 8 (2012) 341.

37 Adegbola A, Lutz R, Nikkola E, Strom SP, Picker J & Wynshaw-Boris A, Disruption of CTNND2, encoding delta-catenin, causes a penetrant attention deficit disorder and myopia. *Hum Genet Genom Adv,* 1 (2020) 1.

38 Woike D, Tibbe D, Hassani Nia F, Martens V, Wang E, Barsukov I & Kreienkamp HJ, The Shank/ProSAP N-Terminal (SPN) Domain of Shank3 Regulates Targeting to Postsynaptic Sites and Postsynaptic Signaling. *Mol Neurobiol,* 61 (2024) 693.

39 Perfitt TL, Wang X, Dickerson MT, Stephenson JR, Nakagawa T, Jacobson DA & Colbran RJ, Neuronal L-type calcium channel signaling to the nucleus requires a novel CaMKIIα-Shank3 interaction. *J Neurosci,* 40 (2020) 2000.

40 Robison A, Emerging role of CaMKII in neuropsychiatric disease. *Trends Neurosci,* 37 (2014) 653.

41 Mameza MG, Dvoretskova E, Bamann M, Hönck HH, Güler T, Boeckers T M, Schoen M, Verpelli C, Sala C & Barsukov I, SHANK3 gene mutations associated with autism facilitate ligand binding to the Shank3 ankyrin repeat region. *J Biol Chem,* 288 (2013) 26697.

42 Salomaa S I, Miihkinen M, Kremneva E, Paatero I, Lilja J, Jacquemet G, Vuorio J, Antenucci L, Kogan K & Nia FH, SHANK3 conformation regulates direct actin binding and crosstalk with Rap1 signaling. *Curr Biol,* 31 (2021) 4956.

43 Bucher M, Niebling S, Han Y, Molodenskiy D, Nia FH, Kreienkamp HJ, Svergun D, Kim E, Kostyukova AS, Kreutz MR & Mikhaylova M, Autism-associated SHANK3 missense point mutations impact conformational fluctuations and protein turnover at synapses. *Elife*, 10 (2021) 1.

44 Kabsch W & Sander C, Dictionary of protein secondary structure: pattern recognition of hydrogen-bonded and geometrical features. *Biopolymers*, 22 (1983) 2577.

45 Katiyar K, Srivastava RK, Nath R & Singh G, Cryptosporidiosis, a public health challenge: A combined 3D shape-based virtual screening, docking study, and molecular dynamics simulation approach to identify inhibitors with novel scaffolds for the treatment of cryptosporidiosis. *Indian J Biochem Biophys,* 59 (2022) 296.

46 Krieger E, Koraimann G & Vriend G, Increasing the precision of comparative models with YASARA NOVA—a self-parameterizing force field. *Proteins,* 47 (2002) 393.

47 Çakmak Ş & Erdoğan T, Some bis (3-(4-nitrophenyl) acrylamide derivatives: Synthesis, characterization, DFT, antioxidant, antimicrobial properties, molecular docking and molecular dynamics simulation studies. *Indian J Biochem Biophys,* 60 (2023) 209.